four parameters, where $C_{p\varepsilon 1}$ is the model coefficient, η is the fraction of the area covered with trees, α is the leaf area density, C_f is the drag coefficient. As model coefficients in turbulence modeling for prescribing the time scale of the process of energy dissipation in the canopy layer, $C_{p\varepsilon 1}$ is given to its appropriate value in this study. However, η, α and C_f are the parameters required to be determined according to the real conditions of trees. (Mochida et al. 2008) calculate the results by using the canopy model when $C_{p\varepsilon 1}$ is 1, 1.5, 1.8, 2, and then compare the predicted results with the measurement data. It is found that the results with $C_{p\varepsilon 1}=1.8$ are in good agreement with the measured data.

A theoretical method is used to derive the model of additional source term S_ω. Based on the relationship between ε and ω: $\varepsilon = C_\mu \omega k$ (C_μ is turbulence parameter), which is taken into the ε equation of the standard $k-\varepsilon$ turbulence model, through the expansion and linear transformation and subtracting k equation, and then compared with the ω equation of the $k-\omega$ turbulence model. The relation formula of the additional source terms of the ω equation is obtained as follows:

$$S_\omega = \left(\frac{S_\varepsilon}{C_\mu \omega} - S_k\right)\frac{\omega}{k} \qquad (7)$$

Substituting S_ε and S_k into the model, the expression of S_ω is obtained:

$$S_\omega = \eta C_f \alpha (C_{p\varepsilon 1} - 1)\frac{\omega}{k} U^3 \qquad (8)$$

2.4 Boundary Conditions and Solution Settings

The boundary conditions are set as follows: the side of the convergence region is a *velocity-inlet* with measured tangential and radial velocity of Spencer tornado; the bottom of convergence region and the side of convection region are set as a no-slip *wall*, and the *outflow* boundary is adopted in the outflow region.

The commercial CFD code “Fluent” was employed to perform 3-D simulations of evolution law of tornado field. The Pressure-Based steady solver is used for the present simulations. The SIMPLE algorithm is used to calculate the coupling between the pressure and velocity fields (Ferziger and Peric, 2002). The turbulence flow in the tornado is calculated by SST k-ω turbulence model. The first-order upwind scheme is employed for the momentum discretization because of it is able to better match the accuracy of the radar, and the pressure space discrete format is adopted PRESTO! format.

3. RESULTS and Discussion

The vegetation, hills and other obstacles on the ground will affect the movement route and speed of wind. According to the characteristics of landscape, supposing that the leaf density of vegetation α is 0.05, the degree of density is 7% of real rough ground in Spencer town.

3.1 Tangential Velocity Distribution

The contour of tangential velocity at the vertical section (y=0) in tornado field is shown in Fig. 2. It can be clearly found that the profile of the tangential velocity in the region near left and right inlet is increased gradually with increasing the height. The tangential velocity reached its minimum value, which is close to 0, in the core region of the tornado. With the increase of radius, the tangential velocity is increased firstly and then decreased. The maximum tangential velocities at different heights are between 100 meter and 200 meter, thus, the core radius can be determined. Below the height of 400 meters above the ground, the maximum tangential velocity at different heights is decreased gradually with the increase of the height, and the core radius increase with the increase of height, and the core radius is increased with the increase of height.

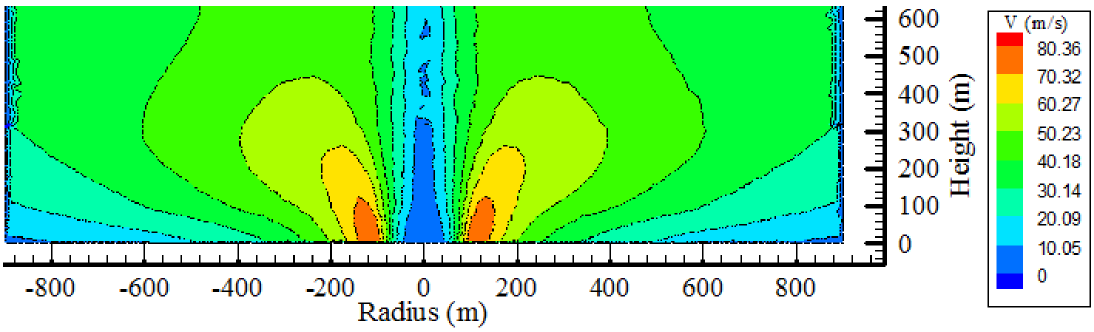

Fig. 2 Contour of tangential velocity at vertical section (y=0)

The contours of tangential velocity at different heights are shown in Fig. 3. It can be seen that the tangential velocity is increased from the center of the wind field to the core radius, and then decreased with increase of the distance out of core radius. At the same time, the maximum tangential velocity at different heights is shown a clear trend of decrease with increase of the height.

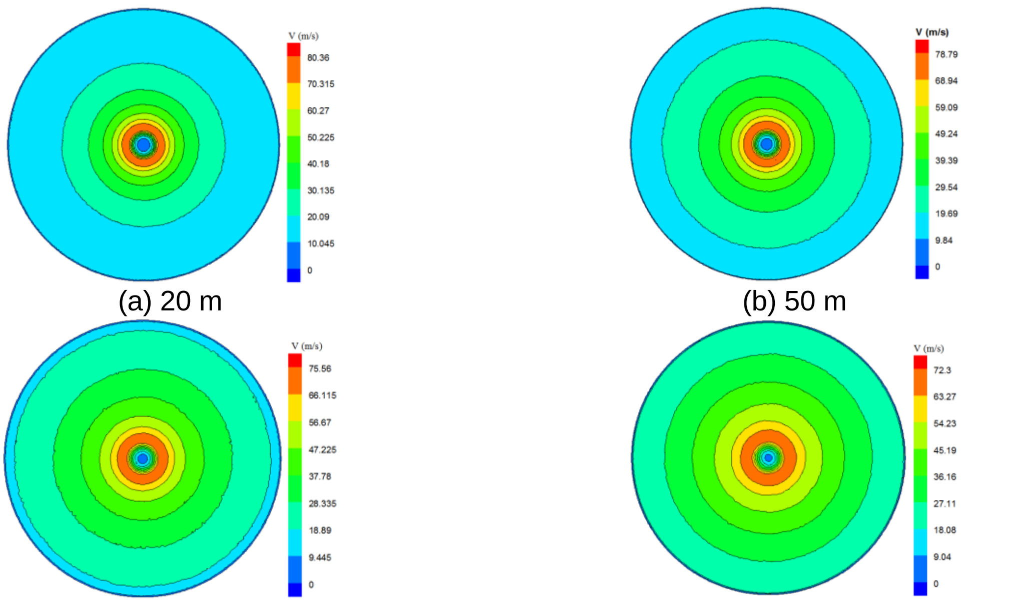

(a) 20 m (b) 50 m

(c) 80 m (d) 110 m

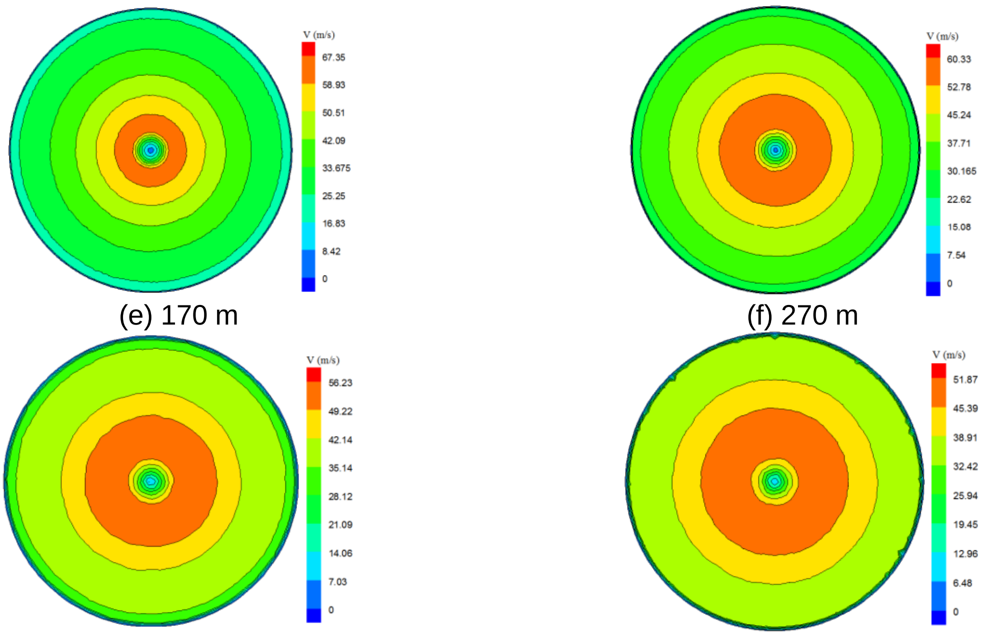

(e) 170 m (f) 270 m

(g) 320 m (h) 420 m

Fig. 3 Contour of tangential velocity at different heights above the ground

3.2 Pressure Distribution

The change of pressure along with the radius is given in Fig. 4(a). As seen in the figure, the larger negative pressure exists in the core region of the tornado, and the pressure distribution at each height is not quite different. When radius $R < 70\,\mathrm{m}$, the pressure did not change significantly and kept at about 7400 Pa. When the radius increases to 200 m, the negative pressure is decreased sharply to about -2000 Pa, and as the radius is further increased, the negative pressure is decreased gradually and finally is closed to about -500 Pa. From the view of pressure versus radial coefficient, which is ratio of the radius to the core radius of different height, it is found that the pressure is changed significantly within 2 times of the core radius. Compared with the pressure calculated by the Rankine vortex theory, the difference of pressure in the center of core region is less than 6%, see Fig. 4(b).

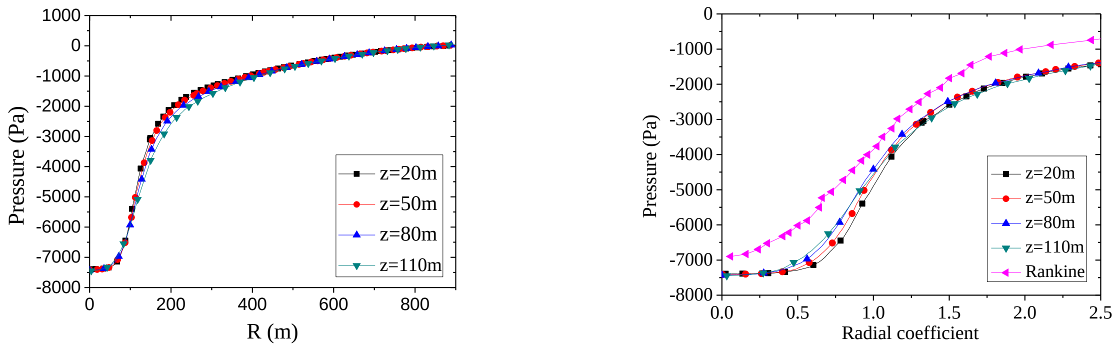

(a) Pressure versus radial (b) Pressure versus radial distribution

Fig. 4 Pressure at different heights in radial directions

3.3 Comparison of Numerical Results and Radar Measured Data

Fig. 5(a) and (b) present the radial profile of tangential velocity at different heights of numerical simulation and radar measurement. At height of 20 meter and 50 meter, the maximum tangential velocity and the core radius are in agreement with the measured data as shown in Tab 2. With the increase of the height, the core radius is gradually increased, while the tangential velocity is become smaller. The present maximum tangential velocity is consistent with that of the radar measurement as shown in Fig. 6. The result shows good consistency between the numerical simulation results and radar measurement.

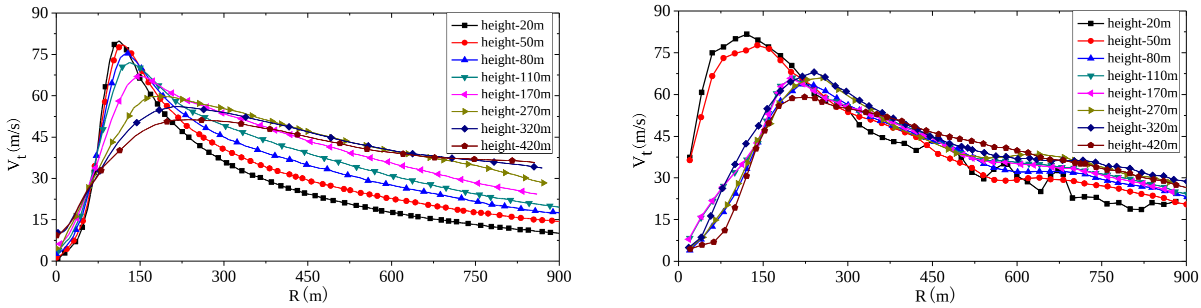

(a) Present (b) Radar measurement

Fig. 5 Comparison of radial profile of tangential velocity between present simulation and the measured data of Spencer tornado

Table 2 Comparison between present results and radar measured data

Height (m)	Core radius of present (m)	Maximum tangential velocity of present (m/s)	Core radius of Radar measurement (m)	Maximum tangential velocity of Radar measurement (m/s)
20	112.33	80.36	110	82
50	119.77	78.79	123	78
80	128.11	75.56	133	76
110	131.17	72.30	145	72
170	146.78	67.35	160	67
270	181.60	60.33	200	60
320	213.95	56.23	216	57
420	236.61	51.87	254	52

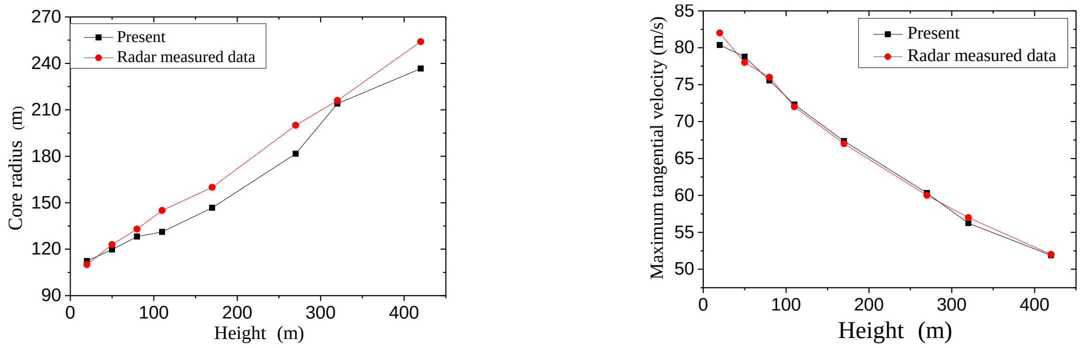

(a) Core radius (b) Tangential velocity

Fig. 6 Comparison between numerical results and radar measured data

4. CONCLUSION

In this study, the tornado-like vortex is generated by a numerical simulator and the effect of ground roughness on the tornado flow field is studied using SST k-ω turbulence model. The following conclusions are summarized.

The effect of vegetation roughness on tornado is performed by adding source term in equation. The tangential velocity and core radius of numerical results are in good agreement with the radar measured data of the Spencer tornado since considering the influence of the roughness. It follows that the structure of tornado-like vortex is affected by the ground roughness. When considering the actual geographical characteristics of the ground, the present full-scale numerical simulator can be used to accurately obtain the wind field characteristics of a tornado.

References

Alexander C R, Wurman J. The 30 May 1998 Spencer, South Dakota, storm. Part l *the structural volution and environment of the tornadoes[J]. Monthly Weather Review*, 2005, **133**(1): 72-97.

Dessens Jr J. Influence of ground roughness on tornadoes: A laboratory simulation *[J]. Journal of Applied Meteorology,* 1972, **11**(1): 72-75.

Diamond C J, Wilkins E M. Translation effects on simulated tornadoes*[J]. Journal of the atmospheric sciences,* 1984, **41**(17): 2574-2580.

Ferziger J, Peric M, 2002. Computational Method for Fluid Dynamics, *3rd ed. Springer, Berlin.*

Ishihara T, Oh S, Tokuyama Y. Numerical study on flow fields of tornado-like vortices using the LES turbulence model*[J]. Journal of Wind Engineering & Industrial Aerodynamics,* 2011, **99**(4): 239-248.

Kuai L, Haan Jr F L, Gallus Jr W A, et al. CFD simulations of the flow field of a laboratory-simulated tornado for parameter sensitivity studies and comparison with field measurements *[J]. Wind and Structures,* 2008, **11**(2): 75-96.

Lewellen D C, Lewellen W S, Xia J. The Influence of a Local Swirl Ratio on Tornado Intensification near the Surface*[J]. Journal of the Atmospheric Sciences,* 2000, **57**(4): 527-544.

Lewellen D C, Lewellen W S. Near-surface intensification of tornado vortices*[J]. Journal of the Atmospheric Sciences,* 2007, **64**(7): 2176-2194.

Lewellen W S, Lewellen D C, Sykes R I. Large-Eddy Simulation of a Tornado's Interaction with The Surface*[J]. Journal of the Atmospheric Sciences,* 1997, **54**(5): 581-605.

Liu Z, Ishihara T. Numerical study of turbulent flow fields and the similarity of tornado vortices using large-eddy simulations*[J]. Journal of Wind Engineering and Industrial Aerodynamics,* 2015, **145**: 42-60.

Liu Z, Ishihara T. Study of the effects of translation and roughness on tornado-like vortices by large-eddy simulations*[J]. Journal of Wind Engineering and Industrial Aerodynamics,* 2016, **151**: 1-24.

Mochida A, Tabata Y, Iwata T, et al. Examining Tree Canopy Models for CFD Prediction of Wind Environment at Pedestrian Level*[J]. Journal of Wind Engineering and Industrial Aerodynamics,* 2008, **96**(10-11): 1667-1677.

Natarajan D, Hangan H. Numerical study on the effects of surface roughness on tornado-like flows*[C]//11th Americas Conference on Wind Engineering (11ACWE).* 2009.

Natarajan D, Hangan H. Large eddy simulations of translation and surface roughness effects on tornado-like vortices*[J]. Journal of Wind Engineering and Industrial Aerodynamics,* 2012, **104**: 577-584.

Wicker L J, Wilhelmso R B. Simulation and Analysis of Tornado Development and Decay Within a Three-Dimensional Supercell Thunderstorm*[J]. Journal of the Atmospheric Sciences*, 1995, **52**(15): 2675-2703.

Zhang W, Sarkar P P. Effects of ground roughness on tornado like vortex using PIV. In: *Proceedings of the AAWE Workshop. Vail, Colorado,* 2008.